A record of aerobic methane oxidation in tropical Africa over the last 2.5 Ma

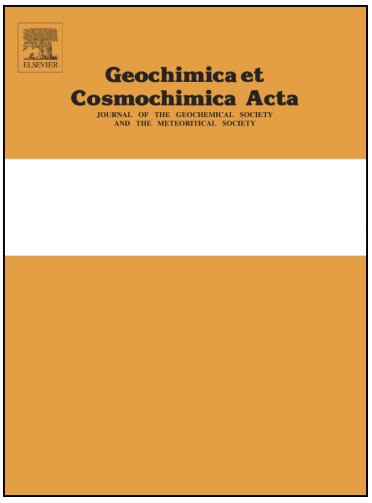

A record of aerobic methane oxidation in tropical Africa over the last 2.5 Ma

Charlotte L. Spencer-Jones, Thomas Wagner, Helen M. Talbot

PII: S0016-7037(17)30545-8
DOI: http://dx.doi.org/10.1016/j.gca.2017.08.042
Reference: GCA 10447

To appear in: *Geochimica et Cosmochimica Acta*

Received Date: 23 September 2016

Please cite this article as: Spencer-Jones, C.L., Wagner, T., Talbot, H.M., A record of aerobic methane oxidation in tropical Africa over the last 2.5 Ma, *Geochimica et Cosmochimica Acta* (2017), doi: http://dx.doi.org/10.1016/j.gca.2017.08.042

A record of aerobic methane oxidation in tropical Africa over the last 2.5 Ma

Charlotte L. Spencer-Jones[a], Thomas Wagner[b,a*], Helen M. Talbot[a]

[a] School of Civil Engineering and Geosciences, Drummond Building, Newcastle University, Newcastle upon Tyne, NE1 7RU, UK

[b] Lyell Centre, Heriot-Watt University, Edinburgh, EH14 4AP, UK

* Corresponding author. Tel.: +44 (0)131 451 3300; *E mail address:* t.wagner@hw.ac.uk (T. Wagner).

Charlotte L. Spencer-Jones[a], *now at:* Department of Geography, Durham University, Durham, DH 1 3LE, UK.

Abstract

Methane and CO_2 are climatically active greenhouse gases (GHG) and are powerful drivers of rapid global warming. Comparable to the Arctic, the tropics store large volumes of labile sedimentary carbon that is vulnerable to climate change. However, little is known about this labile carbon reservoir, in particular the behaviour of high methane–producing environments (e.g. wetlands), and their role in driving or responding to past periods of global climate change. In this study, we use a microbial biomarker approach that traces continental aerobic methane oxidation (AMO) from sedimentary organic matter in deep-sea fan sediments off the Congo River to reconstruct the link between central African methane cycling and continental export during key periods of global Pleistocene warmth. We use 35-amino bacteriohopanepolyols (BHPs), specifically aminobacteriohopane-31,32,33,34-tetrol (aminotetrol) and 35-aminobacteriohopane-30,31,32,33,34-pentol (aminopentol) as diagnostic molecular markers for AMO (CH_4 oxidation markers) and the prevalence of continental wetland environments. BHPs were analysed in sediments from the Congo fan (ODP 1075) dated to 2.5 Ma. High resolution studies of key warm marine isotope stages (MIS) 5, 11 and 13 are included to test the relationship between CH_4 oxidation markers in sediments at different levels of elevated global atmospheric GHG.

This study presents the oldest reported occurrence, to date, of 35-amino BHPs up to 200 meters below sea floor (~2.5 Ma) with no strong degradation signature observed. Low concentrations of CH_4 oxidation markers identified between 1.7 Ma and 1 Ma suggest a reduction in wetland extent in tropical Africa in response to more arid environmental conditions. Correlation of high resolution CH_4 oxidation marker signatures with global atmospheric GHG concentrations during MIS 5, 11 and 13

further emphasize periods of enhanced tropical C cycling. However, subsequent analysis would be required to further extrapolate the relative importance of tropical methane sources as a driver of global methane concentrations during the Pleistocene.

Key words

Pleistocene, Congo, wetland, methane cycle, methanotrophic bacteria, bacteriohopanepolyols

1. INTRODUCTION

During the past century, Earth has experienced a rapid rise in surface temperature with instrumental records showing the past 30 years to have been successively warmer than the previous decades (IPCC, 2013). In parallel with this rise, significant increase in the atmospheric concentrations of greenhouse gasses (GHG) have been recorded, with methane (CH_4) and carbon dioxide (CO_2) being particularly potent GHG and potential drivers of climate change (IPCC, 2013). Changes in atmospheric temperatures and the hydrological cycle have a coupled impact on biogeochemical cycles, including the C cycle. Perturbations in the C cycle could lead to the degradation of vulnerable C sources such as wetlands (IPCC, 2013). While modern elevated atmospheric GHG concentrations are of natural and anthropogenic origins, the source of them in the palaeo-record as a climate and ecosystem regulator remains unclear. Within the modern terrestrial system, wetlands are the largest natural source of CH_4 and are estimated to account for ~70% of all natural emissions (Wuebbles and Hayhoe, 2002) with tropical wetlands (20°N to 30°S) identified as the largest CH_4 producers (Bartlett and Harriss, 1993; Sjogersten et al., 2014). Changes in the extent and volume of tropical methane sources and sinks (i.e. wetlands and atmospheric oxidation), modulated by fluctuations in the hydrological cycle and vegetation feedbacks, have been shown to exert a significant control on atmospheric methane concentrations over the past 800 ka (e.g. Blunier et al., 1995; Loulergue et al., 2008; Singarayer et al., 2011).

Paleoclimate analysis of West African marine sedimentary archives suggests significant variations in continental aridity and humidity during the Pleistocene leading to the destabilisation of vegetation zones (Schefuß et al., 2003). Biomarker and pollen analysis of deep-sea sedimentary archives from North West Africa

reveals major changes in the balance between C_3 and C_4 vegetation, reflecting significant changes in climate during the past 160 ka (Zhao et al., 2003). Furthermore, biomarker and pollen analysis from southwest African margin sediments along a transect of 9 sites from Congo (4°S) to Cape Bush (30°S) reveal an expansion of C_4 plant indicators during Holocene glacial periods, thus indicating a northward expansion of arid zones favouring grass vegetation (Rommerskirchen et al., 2006). While the quantitative impact of habitat expansion on C cycling remains to be resolved, the expansion of mangroves and wetland environments during these warm periods may have resulted in an increased flux in CH_4 and other GHG to the atmosphere. Indeed, ice core records suggest that changes in the strength of tropical CH_4 reservoirs had an important control on the global atmospheric CH_4 budget during the past 800 ka (Petit et al., 1999; Loulergue et al., 2008). However, direct measurements of atmospheric CH_4 concentration beyond 800 ka are not available from ice cores, requiring an independent proxy approach to explore CH_4 dynamics further back in time, and in non-glacial environments. It has been shown that specific biomarker records are powerful proxies for reconstructing C cycling beyond this time period of direct measurements (Talbot et al., 2014).

Bacteriohopanepolyols (BHPs) are highly functionalised pentacyclic triterpenoids produced by many aerobic as well as a number of obligate and facultative anaerobic bacteria (e.g. Rohmer et al., 1984; Talbot et al., 2008; Eickhoff et al., 2013; and references therein). Some BHPs with an amino group at the C-35 position (35-amino BHPs) are thought to be specific indicators of aerobic methane oxidation (AMO) with 35-aminobacteriohopane-31,32,33,34–tetrol (aminotetrol; **II**; Table 1); 35-aminobacteriohopane-30,31,32,33,34-pentol (aminopentol; **III**), unsaturated aminopentol (**IV/V**) and aminopentol isomer (**III'**; van Winden et al., 2012b) being

almost exclusively produced by aerobic methanotrophs (Talbot and Farrimond, 2007; Zhu et al., 2010; van Winden et al., 2012b; Berndmeyer et al., 2013; herafter referred to as CH_4 oxidation markers). CH_4 oxidation markers have been identified in both terrestrial and marine settings, including but not limited to; peatlands (van Winden et al., 2012a; 2012b; Talbot et al., 2016), a stratified post glacial lake in Antarctica (Coolen et al., 2008), and within suspended particulate matter in ocean settings (Blumenberg et al., 2007; Wakeham et al., 2007; Sáenz et al., 2011), modern soils from the Amazon (Wagner et al., 2014) and Congo hinterland (Spencer-Jones et al., 2015), and ancient sediments from the Amazon (Wagner et al., 2014) and Congo (Talbot et al., 2014) fans. However, despite the variety of terrestrial and marine environments where these biomarkers have been found, current research suggests that when found in marine sediments they are primarily of terrestrial origin (Talbot et al., 2014; Wagner et al., 2014; Schefuß et al., 2016), specifically from catchment wetlands (Spencer-Jones et al., 2015). Large scale fluctuations in the concentration of these compounds during warm – humid interglacial periods have been associated with hydrological changes and corresponding fluctuations in wetland extent (Talbot et al., 2014; Schefuß et al., 2016). Furthermore, hydrologically induced variations in Congo wetland systems during the Holocene resulted in the export of pre-aged OM during arid conditions and younger-OM during humid environmental conditions (Schefuß et al., 2016) potentially leading to lags in biomarker export during past glacial (dry) and at the transition to interglacial (humid) Termination conditions. A previous low-resolution study was limited to the first ~1.2 Ma (115.65 meters below sea floor, m.b.s.f) of a Congo deep-sea fan core (ODP 1075) and, therefore, could not resolve some of the short term variability in 35-amino BHP distributions and, thus, AMO cycling during the earlier parts of the Pleistocene (Talbot et al., 2014).

This study expands on previous research by addressing the causes and implications of short- and long term variability in CH_4 oxidation markers in the Congo fan record (Talbot et al., 2014). This study also explores the fluctuations in CH_4 oxidation markers under different, elevated atmospheric GHG concentrations. We first test the stratigraphic suitability of 35-amino BHPs for palaeoclimate reconstructions in ODP 1075 sediments by expanding the record to the core's maximum depth of 201.25 m.b.s.f (~2.5 Ma). Building on this assessment, we introduce high resolution records of CH_4 oxidation marker concentration for marine isotope stages (MIS) 2-6 and 10-13 to address changes in short term variability in terrestrial CH_4 cycling. These intervals include MIS 5 and 11, which are both considered particularly warm stages in the geologic record with approximate durations of 58 ka and 64 ka, respectively (Howard, 1997; Kukla et al., 1997; Spahni et al., 2005). MIS 5 and 11 are characterised as periods of reduced ice volume with an interglacial and multiple interstadials and stadials (Loutre et al., 2003) and may serve as potential analogues for Earth's future climate. BHP distributions of MIS 5 and 11 are contrasted with the intermediate warm period MIS 13 and cool MIS 2, 3, 4, 6, 10, and 12, to further test the sensitivity of the biomarkers to global GHG levels and improve characterisation of short-term transitions in AMO variation during the Pleistocene.

2. MATERIALS AND METHODS

2.1. SITE LOCATION AND SAMPLE DESCRIPTION

The Congo River is the largest river in Africa and the second largest river in the world in terms of drainage basin size (~3.7 x 10^6 Km_2; Runge, 2007; Laraque et al., 2009) and supplies freshwater, nutrients (including large amounts of SiO_2) and sediment to the ocean. The Congo River plume extends 800 Km offshore and can be

detected during austral summer when monsoon/precipitation reach their maximum seasonal intensity (Anka and Séranne, 2004). The rapid outflow of the Congo River is caused by the relatively small river mouth and a large canyon head (Berger et al., 2002). As a result of coastal, oceanic and river induced upwelling, modern primary production is very high in the surface waters off the Congo continental margin (Anka and Séranne, 2004).

Sedimentation within the Congo fan is dominated by rainout of suspended clays derived from the Congo River and by pelagic settling of biogenic debris (Berger et al., 2002). The lower Congo basin sediments lack a significant river borne sand and silt fraction, due to most of the coarse debris being deposited before it reaches the ocean (Spencer et al., 2012).

The Congo catchment hosts extensive wetland and water dependent ecosystems and supports one of the world's largest swamp forests (360 000 Km^2; Bwangoy et al., 2010). One prominent example is Malebo Pool, located on the main stem of the Congo River (Fig. 1). Organic matter (OM) exported from this region has been shown to be geochemically very similar to OM at the head of the estuary (~ 350 km downstream), consistent with no major tributaries joining the Congo River between Malebo Pool and the Atlantic Ocean (Spencer et al., 2012). Annual water level change in Malebo Pool is ~3 m and average river flow is ~30 000 $m^3 s^{-1}$ during dry periods and 60 000 $m^3 s^{-1}$ during the wet season (Thieme et al., 2005).

During the Ocean Drilling Program (ODP) leg 175, 13 sites were drilled off the West African coast (Aug-1997; Shipboard Scientific Party, 1998). ODP site 1075 is a deep water drill site on a depth transect in the lower Congo basin located at 2995 m water depth. ODP 1075 is dominated by (1) freshwater input from the Congo River, (2)

seasonal coastal upwelling activity and associated filaments and eddies moving offshore, and (3) incursions of open-ocean waters from the South Equatorial Countercurrent (Berger et al., 2002). Sediments from ODP 1075 and neighboring cores (e.g. ODP 1077) have been closely correlated with climatic signaling (Jahn et al., 2005) and large scale shifts in terrestrial vegetation relating to humidity – aridity cycles (Dupont et al., 2000; Schefuß et al., 2003; 2004). ODP 1075 is approximately 200 m.b.s.f. with an average sedimentation rate of 100 m/Ma. OM in ODP 1075 is of mixed terrestrial and marine origin, with soil OM (SOM) being an important but variable contributor (Holtvoeth et al., 2001, 2003).

Sediment cores from ODP 1075 were stored at the International Ocean Discovery Program (IODP) Bremen Core Repository (MARUM, Bremen University) at 4°C. Samples between 1.65 and 115.65 m.b.s.f were previously collected by Holtvoeth et al. (2001) and made available to this study. The lower section between 115.7-201.25 m.b.s.f of ODP 1075 (core A) were re-sampled at 1 m intervals, resolving on average 13 to 18 ka. The samples were stored in polypropylene bags and shipped to Newcastle University (UK) where they were frozen immediately upon arrival.

2.2. STRATIGRAPHY AND AGE MODEL

Stratigraphy and the age model of ODP 1075 was previously determined by Dupont et al. (2001). Due to low amounts of calcareous foraminifera in ODP 1075 for oxygen isotope stratigraphy, the age model was established by correlating magnetic susceptibility of 1075 with the neighboring site 1077. Both ODP sites 1075 and 1077 represent the same hydrographic conditions and show similar variations in magnetic susceptibility (see Fig. 1 in Dupont et al., 2001). The age model for site 1077 is based on a correlation of the $\delta^{18}O$ curve for *Globigerinoides ruber* (pink) with the benthic isotope record of ODP site 677 in the deep Pacific (Shackleton et al., 1990).

Sedimentation rates were calculated by linear interpolation between age control points (Jahn, 2002). The error associated with the age model of ODP 1075 has been roughly estimated by Berger et al. (2002) to be approximately 0.01 Ma. The age assignment of MIS are according to Lisiecki and Raymo (2005).

2.3. TOTAL ORGANIC CARBON (TOC)

Total OC (%) content of ODP 1075 samples between 115.7-201.25 m.b.s.f were measured at Newcastle University using a LECO CS244 Carbon/Sulfur Analyser as detailed in Spencer-Jones et al. (2015). TOC of samples between 1.65-115.65 m.b.s.f were obtained from Holtvoeth et al. (2003).

2.4. LIPID EXTRACTION

Total lipids were extracted using an adaptation of the method published in Talbot et al. (2007) and further modified by Osborne (2016), which is based on the Kates modification (Kates, 1972) of the Bligh and Dyer extraction (Bligh and Dyer, 1959). Total lipids were extracted from 1-3 g of freeze-dried and homogenised sediment. Sediment was extracted in a Teflon centrifuge tube (50 ml) with a monophasic mixture of bi-distilled water (4 ml), methanol (10 ml) and chloroform (5 ml). The sample was agitated vigorously via sonication for 15 min at 40ºC followed by centrifugation for 15 min at 12000 rpm. The supernatant was collected and added to a second 50 ml centrifuge tube. This extraction was repeated three times with the supernatant collected at the end of each extraction cycle.

The monophasic extracts were phase separated via addition of chloroform (5 ml) and bi-distilled water (5 ml) to each of the supernatants. The sample was gently inverted and centrifuged for 5 minutes (12000 rpm) to break the emulsion. The organic layer from each tube was transferred to a round bottom flask (100 ml) and concentrated

using a rotary evaporator. The total lipid extract (TLE) was transferred to a glass vial using chloroform/methanol at a ratio of 2:1 (v/v). A 5α-pregnane-3β,20β-diol internal standard was added to the TLE. One third of the TLE was acetylated using acetic anhydride (250 µl) and pyridine (250 µl). The TLE was heated at 50ºC for one hour and then left at room temperature overnight. Samples were dried under a stream of N_2 with heating from below (40ºC). BHP extracts were then stored at 4ºC prior to further processing.

2.5. BACTERIOHOPANEPOLYOL ANALYSIS

BHP analysis was performed by HPLC-APCI-MS^n using a ThermoFinnigan surveyor HPLC system fitted with a Phenomenex Gemini C_{18} column (150 mm; 3.0 mm i.d.; 5 µm particle size) and a security guard column cartridge of the same material coupled to a Finnigan LCQ ion-trap mass spectrometer equipped with an APCI source operated in positive ion mode, as described in Talbot et al. (2003). The error in absolute quantification was ± 20%, based on selected replicate analyses and BHP standards of known concentration (Cooke, 2010; van Winden et al., 2012b). The abbreviated names of the compounds identified, characteristic base peak ions (*m/z*) and structure numbers are given (Table 1). All concentrations are given to 2 significant figures with raw data presented in Appendix A. Statistical analysis was performed using Minitab 17.1.0. Spearmans Rho (R_s) correlation index was performed on BHP abundances. "CH_4 oxidation markers" is the sum of aminotetrol, aminopentol, aminopentol isomer, and unsaturated aminopentol (**II**, **III**, **III'**, **IV/V**). In this study, we report 182 new BHP data points from the Congo deep-sea fan (ODP site 1075) which are complemented by 122 data points published by Talbot et al. (2014).

3. RESULTS

Consistent with Talbot et al. (2014), aminotriol (**I**), aminotetrol (**II**), aminopentol (**III**), aminopentol isomer (**III'**), and unsaturated aminopentol (**IV** or **V**) are identified within ODP 1075 sediments (Fig. 2a, b, c, and e). Aminotriol is the most abundant 35-amino BHP with concentrations between 4.6 and 360 µg $gTOC^{-1}$. This is followed by aminopentol as the second most abundant 35-amino BHP with concentrations ranging between 0 and 280 µg $gTOC^{-1}$. Aminotetrol is identified at lower concentrations, compared with aminotriol and aminopentol and is intermittently present throughout ODP 1075. Despite differences in concentration, aminotriol, aminotetrol, and aminopentol show similarities in distributions and persist to the bottom of the core at 201.25 m.b.s.f (~2.5 Ma). In contrast, unsaturated aminopentol (0 and 12 µg $gTOC^{-1}$) and aminopentol isomer (0 and 39 µg $gTOC^{-1}$) are present at much lower concentrations and do not show a similar distribution to aminotriol, aminotetrol and aminopentol (Fig. 2b and c). Significant correlation is found between aminopentol and aminotriol (R_s 0.891, $p<0.05$; Fig. 2e), aminopentol and aminotetrol (R_s 0.908, $p<0.05$; Fig. 2e), and aminotriol and aminotetrol (R_s 0.904, $p<0.05$, not shown), supporting a common response of all compounds to changing environmental and/or depositional conditions. No statistically relevant correlation is observed between TOC and aminotriol (R_s 0.101, p 0.079), aminotetrol (R_s -0.042, p 0.463), or aminopentol (R_s 0.006, p 0.920) concentrations (µg g $sediment^{-1}$; figures not shown). Total CH_4 oxidation marker concentrations (sum **II**, **III**, **III'**, **IV/V**) are highly variable down core (Fig. 2d). Peak concentrations in CH_4 oxidation markers occur at around 1686 ka (270 µg $gTOC^{-1}$), 1271 ka (330 µg $gTOC^{-1}$) and 491 ka (270 µg $gTOC^{-1}$). Starting at the Pliocene/Pleistocene transition (~2.5 Ma), a steady increase in CH_4 oxidation marker concentration is observed. Between 1865 and

1713 ka (hereafter referred to as interval '*a*'; Fig. 2d) a clear decrease in CH_4 oxidation marker concentration is observed. A similar reduction in CH_4 oxidation markers (µg $gTOC^{-1}$) is also observed between 1099 ka and 826 ka (hereafter referred to as interval '*b*'; Fig. 2d).

35-Amino BHPs show a similar distribution within the high resolution sections to the full ODP 1075 record (Fig. 3 and Fig. 4). Aminotriol is the most abundant BHP (4.6 and 270 µg $gTOC^{-1}$) followed by aminopentol (0 and 210 µg $gTOC^{-1}$). Unsaturated aminopentol and aminopentol isomer have an intermittent presence between MIS 2-6 and MIS 10-13. Peak concentrations in aminotriol, aminotetrol, and aminopentol are observed during MIS 5, 11, and 13, reaching comparable maximum levels for all three warm intervals (Fig. 3 and Fig. 4). Similar to the overall BHP distribution in ODP 1075 (Fig. 2), CH_4 oxidation marker concentrations are highly variable during the investigated high resolution MIS intervals (Fig. 3 and Fig. 4). High concentrations of total CH_4 oxidation markers are observed during MIS 13 (range 0 and 270 µg $gTOC^{-1}$, mean 130 µg $gTOC^{-1}$), followed by a reduction during MIS 12 (range 0 and 210 µg $gTOC^{-1}$, mean 51 µg $gTOC^{-1}$), and a marked increase in CH_4 oxidation markers during MIS 11 (range 0 and 260 µg $gTOC^{-1}$, mean 96 µg $gTOC^{-1}$). Peak concentration in CH_4 oxidation marker is similar during MIS 11 and 13 (Fig. 3). Low concentrations of CH_4 oxidation markers are observed during MIS 6 (range 0 and 39 µg $gTOC^{-1}$, mean 14 µg $gTOC^{-1}$) followed by an increase in concentration during MIS 5 (range 5.7 and 190 µg $gTOC^{-1}$, mean 66 µg $gTOC^{-1}$). Following MIS 5, CH_4 oxidation marker concentration remains low during MIS 2-4 (range 0 and 96 µg $gTOC^{-1}$, mean 14 µg $gTOC^{-1}$). Overall higher mean CH_4 oxidation markers are observed during MIS 11 and 13 compared with MIS 5 (Fig. 5).

4. DISCUSSION

4.1. DIAGENETIC AND ENVIRONMENTAL CONTROLS ON 35-AMINO BHPS IN ODP 1075

Aminotriol (**I**), aminotetrol (**II**) and aminopentol (**III**) down core profiles do not show clear diagenetic trends, with all of these compounds present within ODP 1075 sediments dated to ~ 2.5 Ma (Fig. 2). The absence of any correlation between TOC and 35-amino BHP suggests that variations in BHPs are not driven by variations in TOC. One previous study exists discussing the preservation of 35-amino BHPs in ancient sediments, where Wagner et al. (2014) identified CH_4 oxidation markers in Amazon fan and shelf sediments to a maximum core depth of 708 cm, dated to approximately 30 ka. The results shown here from the Congo deep-sea fan represent the oldest and longest continuous record of CH_4 oxidation markers in sediments to date. As no clear diagenetic trend in CH_4 oxidation markers is evident we anticipate that these biomarkers can be examined within much deeper sediments, without any reasonable justification for a specific sub-surface limit. Furthermore, we also report the occurrence of unsaturated aminopentol and aminopentol isomer within sediments dating to 2.2 Ma and 2.4 Ma, respectively (Fig. 2). The observation of unsaturated aminopentol and aminopentol isomer in ODP 1075, again, is the oldest reported occurrence of these two compounds, building confidence that the high resolution 35-amino BHP records presented here represent primary signals, with minimal or no diagenetic alteration.

Previous analysis of 35-amino BHPs within Congo fan sediments suggest that these compounds are of allochthonous origins, likely derived from Congo hinterland wetlands and similar environments (Talbot et al., 2014). In agreement with previous studies, BHP concentrations and proportions of aminotriol:aminopentol:aminotetrol in

our extended ODP 1075 record show strong correlation to each other (Fig. 2e; Cvejic et al., 2000; Talbot et al., 2001; van Winden et al., 2012b; Osborne, 2016) supporting a common methanotroph source.

4.2. A 2.5 MA RECORD OF CH_4 CYCLING

As discussed in Talbot et al. (2014), analysis of Congo fan sediments suggests long term fluctuations in CH_4 oxidation markers during the Pleistocene with enhanced production and preservation of CH_4 oxidation markers during warm-humid interglacial MIS. The data presented here, support and further expand this concept. Intervals '*a*' and '*b*' (Fig. 2d), suggest a shift in the terrestrial BHP producing community and thus widespread change in African ecology and hydrology that coincides with increased African climate variability and aridity between 1.7 Ma and 1 Ma (deMenocal, 2004; Trauth et al., 2007). We propose that increased continental African aridity would have reduced wetland extent and, subsequently, reduced the production and supply of CH_4 oxidation markers to the Congo fan. These arid intervals of low CH_4 oxidation marker concentrations are consistent with the onset and amplification of high latitude glacial conditions (deMenocal et al., 1993, 1995; Tiedemann et al., 1994; Clemens et al., 1996). Furthermore, CH_4 oxidation markers have been shown to follow a systematic pattern of elevated concentrations during warm MIS 5, 11, 13, 17, 21, and 33 (Talbot et al., 2014). Our study further supports this trend and shows that this relationship persists beyond 1.2 Ma to 2.5 Ma with high concentrations of CH_4 oxidation markers identified during MIS 39, 47, 49, 59, 75, and 83 (Fig. 2). This new data further suggests enhanced methane cycling during warm-humid time periods of the Pleistocene.

4.3. SHORT TERM TRENDS IN CH_4 CYCLING

Throughout the Pleistocene, subtropical African climate periodically oscillated between wet and dry climate conditions, which drove largescale ecological change (Schefuß et al., 2003, 2005; deMenocal, 2004). The high resolution timeseries of MIS 5, 11, and 13 show high concentrations of CH_4 oxidation markers, consistent with high global GHG concentrations (Fig. 3 and 4) and suggest enhanced C cycling during these intevals. Furthermore, high concentrations of these biomarkers coincide with the expansion of tropical rainforests and water-dependent ecosystems (Miller and Gosling, 2014) supporting the concept that CH_4 oxidation markers may actually document widespread ecological change in the Congo.

Global methane concentrations were high during MIS 5 and MIS 11 (Fig. 3 and 4) and slightly lower during MIS 13, largely owing to a cooler climate (Spahni et al., 2005). However, the range of CH_4 oxidation marker concentrations in the Congo core are comparable for all three time slices (Fig. 3 and 4), suggesting either similarities in methanotrophy/ecosystem and/or a decoupling between BHP synthesis and aerobic methanotrophy.

4.3.1. WEST AFRICAN ECOSYSTEM DURING THE PLEISTOCENE

Similarities in methanotrophy/ecosystem during MIS 5, 11, and 13 are supported by integrated palynological evidence from various sediment cores from the wider West African coastal area suggesting strong similarities in vegetation, habitat types, and interpreted temperatures and precipitation (Miller and Gosling, 2014). Furthermore, fluctuations in global atmospheric CH_4 concentrations may have been due to changes in Northern hemisphere methane sources (Froese et al., 2008; Vaks et al., 2010; Vázquez Riveiros et al., 2013; Reyes et al., 2014), therefore not directly affecting tropical wetland sources and thus BHP signatures in deep-sea fan settings.

Low concentrations of CH_4 oxidation marker are observed during MIS 2, 3, 4, 6, 10, 12, which also coincides with globally low concentrations of atmospheric GHG and would support the development of dry-arid conditons (Spahni et al., 2005), with restricted extent of water dependent ecosystems (Dalibard et al., 2014). While wetland ecosystems are not well represented within the palynological archive, pollen records can indicate ecosystem community structure and potential environmental conditions (for example, Miller and Gosling, 2014). Limited evidence from pollen records from the tropical Atlantic off West Africa indeed indicates that vegetation assemblages of the Congo basin and surrounding mountains were suceptible to changes in precipitation during the Pleistocene, with extensive rainforest and mangrove ecosystems common during humid stages (Dalibard et al., 2014). The development of more open, savannah-type ecosystems is characteristic of glacial periods (Dupont et al., 2000; Versteegh et al., 2004; Dupont, 2009), suppporting our conculsion of a reduction in wetland habitats during these overall dryer periods.

Progressively lower mean CH_4 oxidation marker concentrations are observed during MIS 5 compared with the older warm isotope stages (i.e. MIS 11 and 13; Fig. 5). This is despite MIS 5 being considered a very warm interglacial with high global atmospheric methane concentrations (Spahni et al., 2005; Loulergue et al., 2008). This disparity may suggest more extended wetlands during MIS 11, 13, and potentially earlier interglacial climate stages of the Pleistocene, compared to MIS 5. Terrestrial and marine paleoclimate records from Africa suggest a trend towards greater aridity during the Pleistocene (Schefuß et al., 2003; deMenocal, 2004; Ségalen et al., 2007; Trauth et al., 2009) consistent with shifts in vegetation from C3 (trees and shrubs) to C4 (tropical grasses). However, despite the global trend towards greater aridity, regional/local trends may have diverged showing more

pronounced variability and higher frequency alternating between dry and humid periods (e.g. Johnson et al., 2016).

4.3.2. DECOUPLING OF BHP SYNTHESIS AND GLOBAL GREENHOUSE GAS CONCENTRATIONS

In addition to climatological and hydrological driven changes in Congo carbon cycling, CH_4 oxidation marker concentrations could also show a potential decoupling between aerobic methanotrophy, BHP synthesis, and atmospheric GHG concentrations. Support for this concept comes from incubations of enrichment cultures that show temperature variations having a strong control on AMO intensity, with peak methane oxidation occurring between 20 and 40°C (van Winden, 2011; Sherry et al., 2016) and resulting in a shift in methanotroph community structure (e.g. Sherry et al., 2016). Furthermore, aerobic methanotroph activity appears closely controlled by the heterogeneity in the soil environment, the solubility and bioavailability of methane - a direct variable linked to methane production and methane flux - and other environmental parameters (e.g. pH, salinity; Sherry et al., 2016). Climate and hydrology cycles were highly variable during the Pleistocene, with MIS 13 relatively cool and arid and MIS 5 and 11 relatively warm and humid (Spahni et al., 2005). These differences could have resulted in differences in carbon cycling and resulted in the BHP concentrations observed in Fig. 2, 3, and 4. Under the warm and humid environmental conditions of MIS 5 and 11, the ecosystem would have supported extended wetlands with intense methanogenesis. Aerobic methanotrophy could have decreased through a potential reduction in the oxic-anoxic boundary or through the methanotroph community being bypassed due to the sudden release of methane bubbles (ebullition, e.g. Bastviken et al., 2004) and/or plant mediated transport of methane gas to the atmosphere (Whalen, 2005). The

degree to which these parameters control BHP synthesis as well as preservation within marine sediments is still largely unknown (Jahnke et al., 1999; Poralla et al., 2000; Doughty et al., 2009; Welander et al., 2009; van Winden, 2011).

4.4. TRANSPORT, DEPOSITION, AND AGE OF BHP RECORDS IN THE CONGO DEEP-SEA FAN

We recognise two principal challenges to constrain the sensitivity of CH_4 oxidation markers in the deep-sea fan within the context of West African climate dynamics. These are (1) the mechanisms and locations of aminopentol signal formation and its transport and burial in the deep marine sediments and (2) a robust high resolution stratigraphic framework to place possible mechanisms into the climatic and sedimentological context of the African-Congo catchment/deep-sea fan system. Here, we further discuss these control mechanisms within a conceptual framework for further research.

4.4.1. TRANSPORT AND DEPOSITION OF BHP SIGNAL IN THE CONGO CATCHMENT

Previous endmember analysis suggests that the source of Congo methane oxidation signature may indeed come from the deep interior of the Congo catchment (Spencer-Jones et al., 2015), and is potentially controlled by central African climate evolution (Schefuß et al., 2016). However, the extent to which the biomarker signal is reworked during transport from source environments to the Congo fan is yet to be elucidated. During riverine transport, a large proportion of sediment is trapped on the Cuvette Centrale with a lesser proportion of sediment subsequently trapped at Malebo pool (Laraque et al., 2009; Spencer et al., 2012). Furthermore, the fine particulate organic matter (FPOM, 0.7-63µm) fraction potentially undergoes some

form of extended degradation in the Cuvette Centrale (Laraque et al., 2009; Spencer et al., 2012). However, Spencer et al. (2012) found little evidence to suggest degradation or variation in the FPOM fraction at the mainstem sites before and after Malebo pool on the Congo River. Therefore, it remains unclear to what extent the BHP component of FPOM may be reworked in the Cuvette Centrale prior to delivery on the Congo fan. The biomarker signal may also be influenced by changes in the topography and run-off patterns as the landscape of the catchment evolved throughout the late Quaternary, possibly with more direct export during earlier interglacial phases in comparison to their more recent analogues.

4.4.2. LAGS IN BIOMARKER RESPONSE

For some but not all glacial-interglacial transitions a delay in biomarker response is noted (e.g. transition from MIS 12-11 in Fig. 4). During MIS 11 a decrease in CH_4 oxidation marker concentration is observed at 388 ka which is 15 ka prior to the beginning of MIS 10. This delay appears to be long taking other studies addressing lead-lag relationships in the Congo system into consideration (e.g. Schneider et al., 1995; Zabel et al., 2001; Holtvoeth et al., 2003) therefore we assume that this is a result of uncertainties in the age model during that specific time period (see section 2.2). Schneider et al. (1995) and Dupont et al. (1999) demonstrated that fluctuations in SST, salinity, runoff, upwelling, organic carbon burial and vegetation in the Congo catchment were in phase and highly sensitive to climate forcing at orbital 23- and 100-kyr periodicities, but did not follow the pacing of global ice-volume and glacial stages, emphasizing the relevance of monsoonal impact on tropical climate systems. The response of the terrestrial biome to climate and hydrological change may possibly have resulted in leads and lags in biomarker response on shorter timescales. Holtvoeth et al. (2003) reports a 2-4 ka time shift of bulk organic

geochemical signatures that correspond to the delayed development of vegetation and soil with respect to atmospheric circulation and insolation, however, the absolute duration of the lag remains unclear within the context of the error associated with the age model of ODP 1075 (see section 2.2). This lag is supported by Zabel et al. (2001), who observe lags between the fluctuation in the suspension load of the Niger River and insolation during the Pleistocene where oscillation of solar radiation led variations of the terrigenous composition by ~4100-5100 yr. In addition to the age model limitations between the comparison of GHG and biomarker records, lag time between vegetation build up and rapid warming, and temporary storage (pre-aging) of the terrestrial carbon within the catchment (Schefuß et al., 2016) may also need to be taken into account when interpreting the observed time differences in the GHG and aminopentol records.

5. CONCLUSIONS

35-amino BHPs including aminotriol, aminotetrol and aminopentol are found in high concentrations throughout ODP 1075 to a maximal depth of 201.25 m.b.s.f, equivalent to ~2.5 Ma. This represents the oldest record of 35-amino BHPs and suggests that these biomarkers may well be preserved in much deeper and older sedimentary archives. Low concentrations of CH_4 oxidation markers, identified between 1865 and 1713 ka (‘*a*’) and 1099 and 826 ka (‘*b*’), suggest a reduction in wetland extent in response to more arid tropical African environmental conditions, consistent with a reported increase in climate variability and aridity near 1.7 Ma and 1 Ma. Correlation of high resolution CH_4 oxidation marker signatures with global atmospheric methane concentrations during MIS 5, 11, and 13 further suggests periods of enhanced tropical methane cycling. Furthermore, we observe a decoupling between CH_4 oxidation marker concentrations and atmospheric GHG

concentrations potentially due to a range of physical (West African climate and hydrological cycles) and/or biological parameters impacting on the tropical C cycle. Moreover, subsequent analysis is required to extrapolate the relative importance of tropical methane sources as a driver of global methane concentrations observed in ice core records.

ACKNOWLEDGMENTS

We are grateful for funding from the European Research Council for a starting grant (258734) awarded to H.M.T. for project AMOPROX. We thank the Natural Environment Research Council (NERC) for funding (Grant number NE/E017088/1) and the International Ocean Discovery Program (IODP) for supplying sediments. We also thank F. Sidgwick and P. Green for technical support. We thank the Science Research Investment Fund (SRIF) from the UK HEFCE for funding the purchase of the ThermoFinnigan LCQ ion trap mass spectrometer. We thank Lydie Dupont for constructive feedback. We also thank the associate editor (E. Hornibrook) and three anonymous reviewers for constructive feedback.

References

Anka Z. and Séranne M. (2004) Reconnaissance study of the ancient Zaire (Congo) deep-sea fan (ZaiAngo Project). *Mar. Geol.* **209**, 223-244.

Bartlett K. B. and Harriss R. C. (1993) Review and assessment of methane emissions from wetlands. *Chemosphere* **26**, 261-320.

Bastviken D., Cole J., Pace M. and Tranvik L. (2004) Methane emissions from lakes: Dependence of lake characteristics, two regional assessments, and a global estimate. *Glob. Biogeochem. Cycle* **18** DOI; 10.1029/2004gb002238

Berger W. H., Lange C. B. and Wefer G. (2002) Upwelling history of the Benguela-Namibia system: A synthesis of Leg 175 Results. Available from the World Wide Web: <http://www-odp.tamu.edu/publications/175_SR/synth/synth.htm> [Cited 2015-03-05].

Berndmeyer C., Thiel V., Schmale O. and Blumenberg M. (2013) Biomarkers for aerobic methanotrophy in the water column of the stratified Gotland Deep (Baltic Sea). *Org. Geochem.* **55**, 103-111.

Bligh E. G. and Dyer W. J. (1959) A rapid method of total lipid extraction and purification. *Canadian J. Biochem. Physiol.* **37**, 911-917.

Blumenberg M., Seifert R. and Michaelis W. (2007) Aerobic methanotrophy in the oxic-anoxic transition zone of the Black Sea water column. *Org. Geochem.* **38**, 84-91.

Blunier T., Chappellaz J., Schwander J., Stauffer B. and Raynaud D. (1995) Variations in atmospheric methane concentration during the Holocene epoch. *Nature* **374**, 46-49.

Bwangoy J. R. B., Hansen M. C., Roy D. P., De Grandi G. and Justice C. O. (2010) Wetland mapping in the Congo Basin using optical and radar remotely sensed data and derived topographical indices. Remote Sens. Environ, **114**, 73-86.

Clemens S. C., Murray D. W. and Prell W. L. (1996) Nonstationary phase of the plio-pleistocene Asian monsoon. *Science* **274**, 943-948.

Cooke M. P. (2010) The Role of Bacteriohopanepolyols as Biomarkers for Soil Bacterial Communities and Soil Derived Organic Matter, Civil Engineering and Geoscience. Newcastle University (UK), PhD Thesis.

Coolen M. J. L., Talbot H. M., Abbas B. A., Ward C., Schouten S., Volkman J. K. and Sinninghe Damsté J. S. (2008) Sources for sedimentary bacteriohopanepolyols as revealed by 16S rDNA stratigraphy. *Environ. Microbiol.* **10**, 1783-1803.

Cvejic J. H., Bodrossy L., Kovács K. L. and Rohmer M. (2000) Bacterial triterpenoids of the hopane series from the methanotrophic bacteria *Methylocaldum* spp.: Phylogenetic implications and first evidence for an unsaturated aminobacteriohopanepolyol. *FEMS Microbiol. Lett.* **182**, 361-365.

Dalibard M., Popescu S. M., Maley J., Baudin F., Melinte-Dobrinescu M. C., Pittet B., Marsset T., Dennielou B., Droz L. and Suc J. P. (2014) High-resolution vegetation history of West Africa during the last 145 ka. *Geobios* **47**, 183-198.

deMenocal P. B. (1995) Plio-Pleistocene African climate. *Science* **270**, 53-59.

deMenocal P. B. (2004) African climate change and faunal evolution during the Pliocene-Pleistocene. *Earth Planet. Sci. Lett.* **220**, 3-24.

deMenocal P. B., Ruddiman W. F. and Pokras E. M. (1993) Influence of high- and low-latitude processes on African terrestrial climate: Pleistocene eolian records from equatorial Atlantic Ocean Drilling Program Site 663. *Paleoceanography* **8**, 209-242.

Doughty D. M., Hunter R. C., Summons R. E. and Newman D. K. (2009) 2-Methylhopanoids are maximally produced in akinetes of *Nostoc punctiforme*: Geobiological implications. *Geobiology* **7**, 524-532.

Dupont L. M. (2009) The Congo deep-sea fan as an archive of Quaternary change in Africa and the eastern tropical south Atlantic (a review), in: Kneller, B., Martinsen, O.J., McCaffrey, B. (Eds.), *External Controls on Deep-Water Depositional Systems*. S E P M - Soc Sedimentary Geology, Tulsa, pp. 79-87.

Dupont L. M., Bonner B., Schneider R. and Wefer G. (2001) Mid-Pleistocene environmental change in tropical Africa began as early as 1.05 Ma. *Geology* **29**, 195-198.

Dupont L. M., Jahns S., Marret F. and Ning S. (2000) Vegetation change in equatorial West Africa: Time-slices for the last 150 ka. *Palaeogeogr. Palaeoclimatol. Palaeoecol.* **155**, 95-122.

Dupont, L.M., Schmüser, A., Jahns, S. and Schneider, R. (1999) Marine - terrestrial interaction of climate changes in West Equatorial Africa of the last 190,000 years. Palaeoecology of Africa 26, 61-84.

Eickhoff M., Birgel D., Talbot H. M., Peckmann J. and Kappler A. (2013) Bacteriohopanoid inventory of *Geobacter sulfurreducens* and *Geobacter metallireducens*. *Org. Geochem.* **58**, 107-114.

Froese D. G., Westgate J. A., Reyes A. V., Enkin R. J. and Preece S. J. (2008) Ancient permafrost and a future, warmer arctic. *Science* **321**, 1648.

Holtvoeth J., Wagner T., Horsfield B., Schubert C. J. and Wand U. (2001) Late-quaternary supply of terrigenous organic matter to the Congo deep-sea fan (ODP site 1075): Implications for equatorial African paleoclimate. *Geo-Mar. Lett.* **21**, 23-33.

Holtvoeth J., Wagner T. and Schubert C. J. (2003) Organic matter in river-influenced continental margin sediments: The land-ocean and climate linkage at the Late Quaternary Congo fan (ODP Site 1075). *Geochem. Geophys. Geosyst.* **4**, DOI: 10.1029/2003gc000590.

Howard W. R. (1997) A warm future in the past. *Nature* **388**, 418-419.

IPCC (2013) Climate change 2013: The Physical Science Basis. Contribution of working group I to the fifth assessment report of the intergovernmental panel on climate change, Cambridge university press, Cambridge, United Kingdom and New York, NY, USA.

Jahn B. (2002) Mid to Late Pleistocene Variations of Marine Productivity in and Terrigenous Input to the Southeast Atlantic, Berichte, Fachbereich Geowissenschaften. Universität Bremen. PhD Thesis.

Jahn B., Schneider R. R., Muller P. J., Donner B. and Rohl U. (2005) Response of tropical African and East Atlantic climates to orbital forcing over the last 1.7 Ma, in: Head, M.J., Gibbard, P.L. (Eds.), *Early-Middle Pleistocene Transitions: The Land-Ocean Evidence*. Geological Soc Publishing House, Bath, pp. 65-84.

Jahnke L. L., Summons R. E., Hope J. M. and Des Marais D. J. (1999) Carbon isotopic fractionation in lipids from methanotrophic bacteria II: The effects of physiology and environmental parameters on the biosynthesis and isotopic signatures of biomarkers.

Geochim. Cosmochim. Acta **63**, 79-93.

Johnson, T.C., Werne, J.P., Brown, E.T., Abbott, A., Berke, M., Steinman, B.A., Halbur, J., Contreras, S., Grosshuesch, S., Deino, A., Lyons, R.P., C.A., S., S., S. and Sinninghe Damsté, J.S. (2016) A progressively wetter climate in southern East Africa over the past 1.3 million years. *Nature*. **537**, 220-224.

Kates M. (1972) Techniques of lipidology: isolation, analysis and identification of lipids. North-Holland Publishing Company, Amsterdam.

Kukla G., McManus J. F., Rousseau D. D. and Chuine I. (1997) How long and how stable was the last interglacial? *Quat. Sci. Rev.* **16**, 605-612.

Laraque A., Bricquet J. P., Pandi A. and Olivry J. C. (2009) A review of material transport by the Congo River and its tributaries. *Hydrol. Process.* **23**, 3216-3224.

Lisiecki L. E. and Raymo M. E. (2005) A Pliocene-Pleistocene stack of 57 globally distributed benthic delta O-18 records. *Paleoceanography* **20**, DOI: 10.1029/2004pa001071.

Loulergue L., Schilt A., Spahni R., Masson-Delmotte V., Blunier T., Lemieux B., Barnola J.-M., Raynaud D., Stocker T. F. and Chappellaz J. (2008) Orbital and millennial-scale features of atmospheric CH_4 over the past 800,000 years. *Nature* **453**, 383-386.

Loutre M. F. and Berger A. (2003) Marine Isotope Stage 11 as an analogue for the present interglacial. *Global Planet. Change* **36**, 209-217.

Lüthi D., Le Floch M., Bereiter B., Blunier T., Barnola J. M., Siegenthaler U., Raynaud D., Jouzel J., Fischer H., Kawamura K. and Stocker T. F. (2008) High-resolution carbon dioxide concentration record 650,000-800,000 years before present. *Nature* **453**, 379-382.

Miller C. S. and Gosling W. D. (2014) Quaternary forest associations in lowland tropical West Africa. *Quat. Sci. Rev.* **84**, 7-25.

Osborne K. A. (2016) Environmental Controls on Bacteriohopanepolyol Signatures in Estuarine Sediment, Civil Engineering and Geoscience. Newcastle University (UK), PhD Thesis.

Poralla K., Muth G. and Härtner T. (2000) Hopanoids are formed during transition from substrate to aerial hyphae in Streptomyces coelicolor A3(2). *FEMS Microbiol. Lett.* **189**, 93-95.

Petit J. R., Jouzel J., Raynaud D., Barkov N. I., Barnola J. M., Basile I., Bender M., Chappellaz J., Davis M., Delaygue G., Delmotte M., Kotlyakov V. M., Legrand M., Lipenkov V. Y., Lorius C., Pepin L., Ritz C., Saltzman E. and Stievenard M. (1999) Climate and atmospheric history of the past 420,000 years from the Vostok ice core, Antarctica. *Nature* **399**, 429-436.

Reyes A. V., Carlson A. E., Beard B. L., Hatfield R. G., Stoner J. S., Winsor K., Welke B. and Ullman D. J. (2014) South Greenland ice-sheet collapse during Marine Isotope Stage 11. *Nature* **510**, 525-528.

Rohmer M., Bouviernave P. and Ourisson G. (1984) Distribution of hopanoid triterpenes in prokaryotes. *J. Gen. Microbiol.* **130**, 1137-1150.

Rommerskirchen F., Eglinton G., Dupont L. and Rullkotter J. (2006) Glacial/interglacial changes in southern Africa: Compound-specific delta C-13 land plant biomarker and pollen records from southeast Atlantic continental margin sediments. *Geochem. Geophys. Geosyst.* **7**, 21.

Runge J. (2007) The Cong River, Central Africa, in: Gupta, A. (Ed.), *Large Rivers: Geomorphology and Management*. Wiley.

Sáenz J. P., Eglinton T. I. and Summons R. E. (2011) Abundance and structural diversity of bacteriohopanepolyols in suspended particulate matter along a river to ocean transect. *Org. Geochem.* **42**, 774-780.

Schefuß E., Eglinton T. I., Spencer-Jones C. L., Rullkötter J., De Pol Holz R., Talbot H. M., Grootes P. M., Schneider R. R. (2016) Hydrologic control of carbon cycling and aged carbon discharge in the Congo River basin. *Nature Geosci **9***, 687-690.

Schefuß E., Schouten S., Jansen J. H. F. and Sinninghe Damsté J. S. (2003) African vegetation controlled by tropical sea surface temperatures in the mid-Pleistocene period. *Nature* **422**, 418-421.

Schefuß E., Schouten S. and Schneider R. R. (2005) Climatic controls on central African hydrology during the past 20,000 years. *Nature* **437**, 1003-1006.

Schefuß E., Versteegh G. J. M., Jansen J. H. F. and Sinninghe Damsté J.S. (2004) Lipid biomarkers as major source and preservation indicators in SE Atlantic surface sediments. *Deep-Sea Res., Part I* **51**, 1199-1228.

Schneider R. R., Müller P. J. and Ruhland G. (1995) Late Quaternary Surface Circulation in the East Equatorial South-Atlantic - Evidence from Alkenone Sea-Surface Temperatures. *Paleoceanography* **10**, 197-219.

Ségalen L., Lee-Thorp J. A. and Cerling T. (2007) Timing of C4 grass expansion across sub-Saharan Africa. *J. Hum. Evol.* **53**, 549-559.

Shackleton N. J., Berger A. and Peltier W. R. (1990) An Alternative Astronomical Calibration of the Lower Pleistocene Timescale Based on Odp Site 677. *T Roy Soc Edin-Earth* **81**, 251-261.

Sherry A., Osborne K. A., Sidgwick F. R., Gray N. D. and Talbot H. M. (2016) A temperate river estuary is a sink for methanotrophs adapted to extremes of pH, temperature and salinity. *Environ. Microbiol. Rep.* **8**, 122-131.

Shipboard Scientific Party (1998). Proceedings of the Ocean Drilling Program, Initial Reports, 175. Ocean Drilling Program, College Station, Texas.

Singarayer J. S., Valdes P. J., Friedlingstein P., Nelson S. and Beerling D. J. (2011) Late Holocene methane rise caused by orbitally controlled increase in tropical sources. *Nature* **470**, 82-91.

Sjogersten S., Black C. R., Evers S., Hoyos-Santillan J., Wright E.L. and Turner B. L. (2014) Tropical wetlands: A missing link in the global carbon cycle? *Global Biogeochem. Cycles* **28**, 1371-1386.

Spahni R., Chappellaz J., Stocker T. F., Loulergue L., Hausammann G., Kawamura K., Fluckiger J., Schwander J., Raynaud D., Masson-Delmotte V. and Jouzel J. (2005) Atmospheric methane and nitrous oxide of the late Pleistocene from Antarctic ice cores. *Science* **310**, 1317-1321.

Spencer R. G. M., Hernes P. J., Aufdenkampe A. K., Baker A., Gulliver P., Stubbins A., Aiken G. R., Dyda R. Y., Butler K. D., Mwamba V. L., Mangangu A. M., Wabakanghanzi J. N. and Six J. (2012) An initial investigation into the organic matter biogeochemistry of the Congo River. *Geochim. Cosmochim. Acta* **84**, 614-627.

Spencer-Jones C. L., Wagner T., Dinga B. J., Schefuß E., Mann P. J., Poulsen J. R., Spencer R. G. M., Wabakanghanzi J. N. and Talbot H. M. (2015) Bacteriohopanepolyols in tropical soils and sediments from the Congo River catchment area. *Org. Geochem.* **89-90**, 1-13.

Talbot H. M. and Farrimond P. (2007) Bacterial populations recorded in diverse sedimentary biohopanoid distributions. *Org. Geochem.* **38**, 1212-1225.

Talbot H. M., Handley L., Spencer-Jones C. L., Bienvenu D. J., Schefuß E., Mann P. J., Poulsen J. R., Spencer R. G. M., Wabakanghanzi J. N. and Wagner T. (2014) Variability in aerobic methane oxidation over the past 1.2Myrs recorded in microbial biomarker signatures from Congo fan sediments. *Geochim. Cosmochim. Acta* **133**, 387-401.

Talbot H. M., McClymont E., Inglis G. N., Evershed E. P., Pancost R. D. (2016) Origine and preservation of bacteriohopanepolyol signatures in *Sphagnum* peat from Bissendorfer moor (Germany). *Org. Geochem.* **97**, 95-110.

Talbot H. M., Squier A. H., Keely B. J. and Farrimond P. (2003) Atmospheric pressure chemical ionisation reversed-phase liquid chromatography/ion trap mass spectrometry of intact bacteriohopanepolyols. *Rapid Commun. Mass Spectrom.* **17**, 728-737.

Talbot H. M., Summons R. E., Jahnke L. L., Cockell C. S., Rohmer M. and Farrimond P. (2008) Cyanobacterial bacteriohopanepolyol signatures from cultures and natural environmental settings. *Org. Geochem.* **39**, 232-263.

Talbot H. M., Watson D. F., Murrell J. C., Carter J. F. and Farrimond P. (2001) Analysis of intact bacteriohopanepolyols from methanotrophic bacteria by reversed-phase high-performance liquid chromatography-atmospheric pressure chemical ionisation mass spectrometry. *J. Chromatogr. A* **921**, 175-185.

Thieme M.L., Abell R., Burgess N., Lehner B., Dinerstein E., Olson D., Teugels G., Kamdem-Toham A., Stiassny M.L.J.S. and Skelton P. (2005) Freshwater Ecoregions of Africa and Madagascar. Island Press, Washington DC.

Tiedemann R., Sarnthein M. and Shackleton N. J. (1994) Astronomic timescale for the Pliocene Atlantic δ18O and dust flux records of Ocean Drilling Program site 659. *Paleoceanography* **9**, 619-638.

Trauth M. H., Larrasoaña J. C. and Mudelsee M. (2009) Trends, rhythms and events in Plio-Pleistocene African climate. *Quat. Sci. Rev.* **28**, 399-411.

Trauth M. H., Maslin M. A., Deino A. L., Strecker M. R., Bergner A. G. N. and Dühnforth M. (2007) High- and low-latitude forcing of Plio-Pleistocene East African climate and human evolution. *J. Hum. Evol.* **53**, 475-486.

Vaks A., Bar-Matthews M., Matthews A., Ayalon A. and Frumkin A. (2010) Middle-Late Quaternary paleoclimate of northern margins of the Saharan-Arabian Desert: reconstruction from speleothems of Negev Desert, Israel. *Quat. Sci. Rev.* **29**, 2647-2662.

van Winden J. F. (2011) Methane Cycling in Peat Bogs: Environmental Relevance of Methanotrophs Revealed by Microbial Lipid Chemistry. LPP Contribution Series (35). Utrecht University.

van Winden J. F., Talbot H. M., De Vleeschouwer F., Reichart G. -J. and Sinninghe Damsté J. S. (2012a) Variation in methanotroph-related proxies in peat deposits from Misten Bog, Hautes-Fagnes, Belgium. *Org. Geochem.* **53**, 73-79.

van Winden J. F., Talbot H. M., Kip N., Reichart G. J., Pol A., McNamara N. P., Jetten M. S. M., den Camp H. and Sinninghe Damsté J. S. (2012b) Bacteriohopanepolyol signatures as markers for methanotrophic bacteria in peat moss. *Geochim. Cosmochim. Acta* **77**, 52-61.

Vázquez Riveiros N., Waelbroeck C., Skinner L., Duplessy J. C., McManus J. F., Kandiano E. S. and Bauch H. A. (2013) The "MIS 11 paradox" and ocean circulation: Role of millennial scale events. *Earth Planet. Sci. Lett.* **371-372**, 258-268.

Versteegh G. J. M., Schefuß E., Dupont L., Marret F., Sinninghe Damsté J. S. and Jansen J. H. F. (2004) Taraxerol and Rhizophora pollen as proxies for tracking past mangrove ecosystems. *Geochim. Cosmochim. Acta* **68**, 411-422.

Wagner T., Kallweit W., Talbot H. M., Mollenhauer G., Boom A. and Zabel M. (2014) Microbial biomarkers support organic carbon transport from methane-rich Amazon wetlands to the shelf and deep sea fan during recent and glacial climate conditions. *Org. Geochem.* **67**, 85-98.

Wakeham S. G., Amann R., Freeman K. H., Hopmans E. C., Jørgensen B. B., Putnam I. F., Schouten S., Sinninghe Damsté J. S., Talbot H. M. and Woebken D. (2007) Microbial ecology of the stratified water column of the Black Sea as revealed by a comprehensive biomarker study. *Org. Geochem.* **38**, 2070-2097.

Welander P. V., Hunter R. C., Zhang L. C., Sessions A. L., Summons R. E. and Newman D. K. (2009) Hopanoids Play a Role in Membrane Integrity and pH Homeostasis in *Rhodopseudomonas palustris* TIE-1. *J. Bacteriol.* **191**, 6145-6156.

Whalen S. C. (2005) Biogeochemistry of methane exchange between natural wetlands and the atmosphere. *Environ. Eng. Sci.* **22**, 73-94.

Wuebbles D. J. and Hayhoe K. (2002) Atmospheric methane and global change. Earth-Sci. Rev. **57**, 177-210.

Zabel M., Schneider R. R., Wagner T., Adegbie A. T., de Vries U. and Kolonic S. (2001) Late Quaternary climate changes in central Africa as inferred from terrigenous input to the Niger fan. Quaternary Research **56**, 207-217.

Zhao M. X., Dupont L., Eglinton G. and Teece M. (2003) n-alkane and pollen reconstruction of terrestrial climate and vegetation for NW Africa over the last 160 kyr. Org. Geochem. 34, 131-143.

Zhu C., Talbot H. M., Wagner T., Pan J. M. and Pancost R. D. (2010) Intense aerobic methane oxidation in the Yangtze Estuary: A record from 35-aminobacteriohopanepolyols in surface sediments. *Org. Geochem.* **41**, 1056-1059.

Table 1. List of 35-amino containing compounds identified in samples with corresponding abbreviated names, structures, and base peak (*m/z*) values. $[M+H]^+$

Compound name	Abbreviated name	Structure	Base peak *m/z*
35-aminobacteriohopane-32,33,34-triol	aminotriol	**I**	714
35-aminobacteriohopane-31,32,33,34–tetrol	aminotetrol	**II**	772
35-aminobacteriohopene-30,31,32,33,34-pentol	unsaturated aminopentol	**IV/V**	828
35-aminobacteriohopane-30,31,32,33,34-pentol	aminopentol	**III**	830
35-aminobacteriohopane-30,31,32,33,34-pentol	aminopentol isomer	**III'**	788

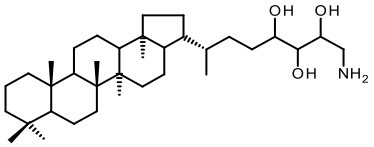

I

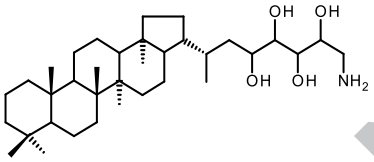

II

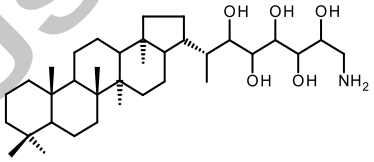

III

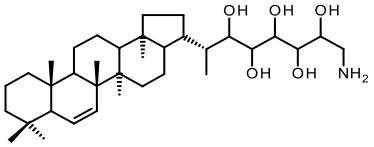

IV

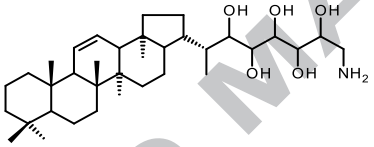

V

Figure 1. Map of Congo including locations of ODP 1075 and Malebo Pool.

Figure 2. Concentration (µg $gTOC^{-1}$) of aminopentol (a), unsaturated aminopentol (b), aminopentol isomer (c), and CH_4 oxidation marker concentration (d) in ODP 1075 from 10 ka to 2.5 Ma, +/- 20% analytical error. In graph d, the black line indicates 3 point rolling average, hatched panel *'a'* represents an interval from 1865-1713 ka and hatched panel *'b'* represents an interval from 1099-826 ka. Correlation between aminopentol (AP) vs. aminotriol (AT) (R_s 0.891, <0.05) and aminopetol vs. aminotetrol (ATT) (R_s 0.908, $P<0.05$) shown in e (insert). Grey bars across a, b, and c indicate selected marine isotope stages (MIS)

Figure 3. A; Global CH_4 (Loulergue et al., 2008; Spahni et al., 2005; black, ppbv) and CO_2 concentrations (Lüthi et al., 2008; grey, ppmv). B; Concentration of CH_4 oxidation markers (µg $gTOC^{-1}$; ODP 1075), from 350 ka to 540 ka. Grey bars indicate MIS 10 and 12.

Figure 4. A; Global CH_4 (Loulergue et al., 2008; Spahni et al., 2005; black, ppbv) and CO_2 concentrations (Lüthi et al., 2008; grey, ppmv). B; Concentration of CH_4 oxidation markers (µg $gTOC^{-1}$; ODP 1075), from 10 ka to 200 ka. Grey bars indicate MIS 2, 4 and 6.

Figure 5. CH_4 oxidation marker concentration (µg $gTOC^{-1}$) during MIS 5 (n=20), 6 (n=8), 10 (n=10), 11 (n=36), 12 (n=38), and 13 (n=21) with median (black line) and mean (grey line) shown on each box.

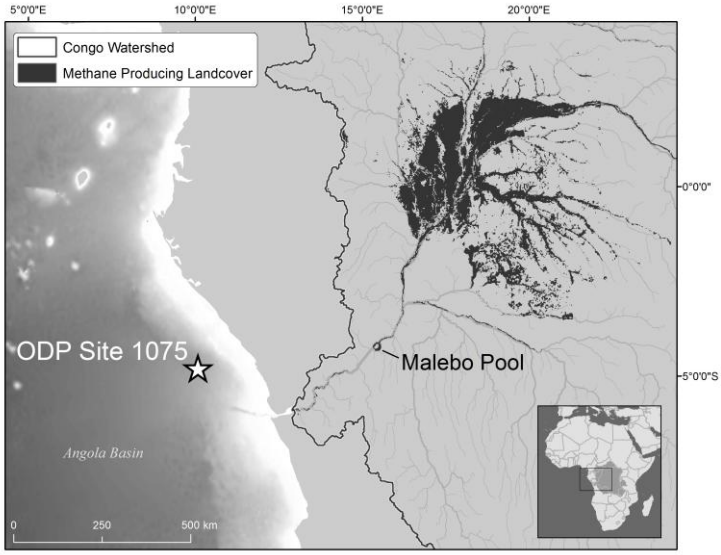

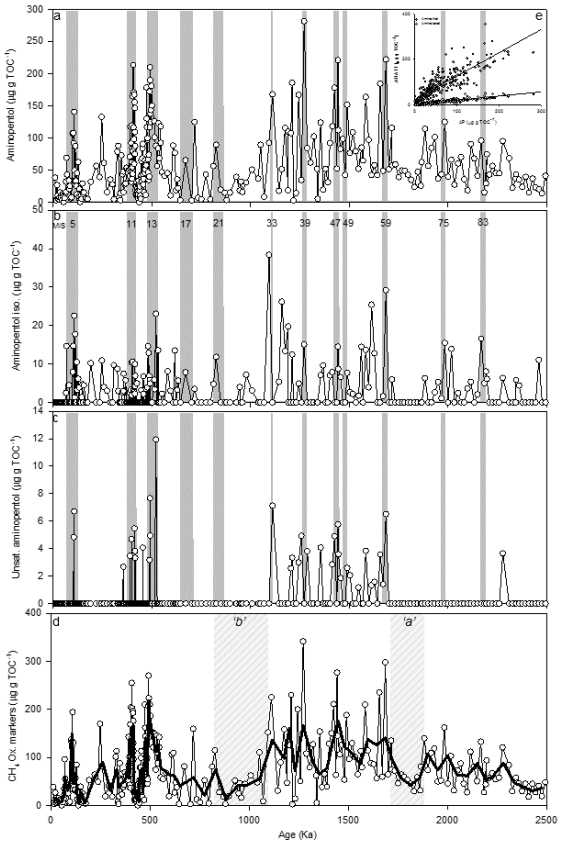
a
e
Aminopentol (µg g TOC⁻¹)
b
MIS 5
11
13
17
21
33
39
47
49
59
75
83
Aminopentol iso. (µg g TOC⁻¹)
c
Unsat. aminopentol (µg g TOC⁻¹)
d
'b'
'a'
CH4 Ox. markers (µg g TOC⁻¹)
Age (Ka)

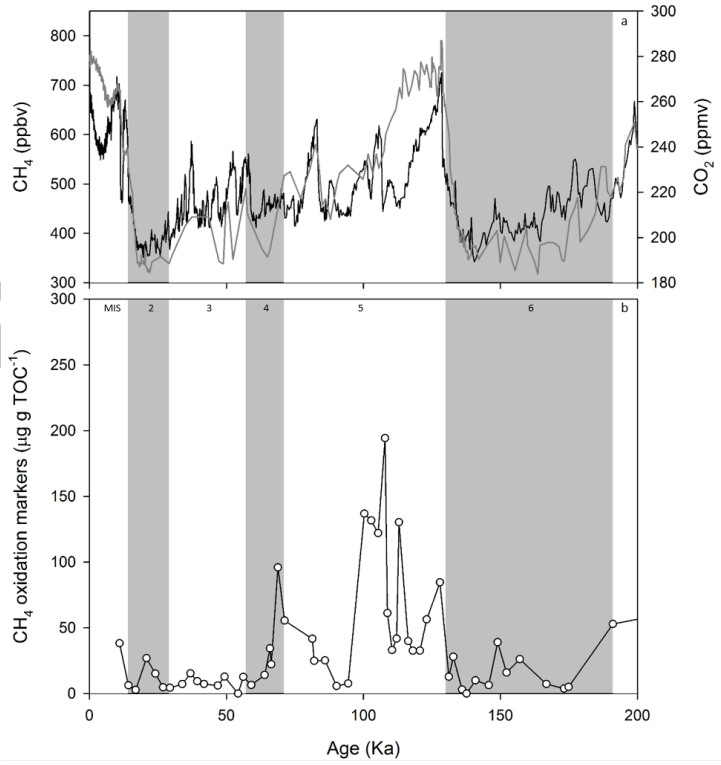
a
CH4 (ppbv)
CO2 (ppmv)
MIS
2
3
4
5
6
b
CH4 oxidation markers (µg g TOC⁻¹)
Age (Ka)

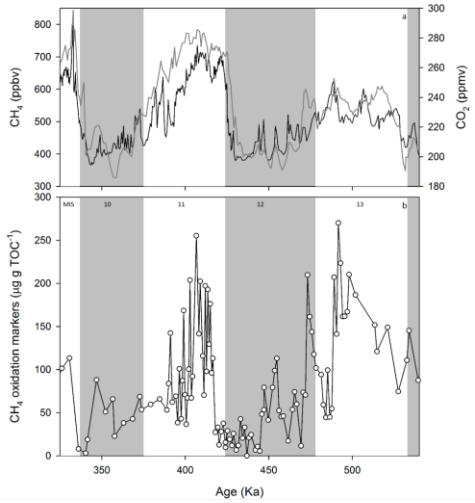

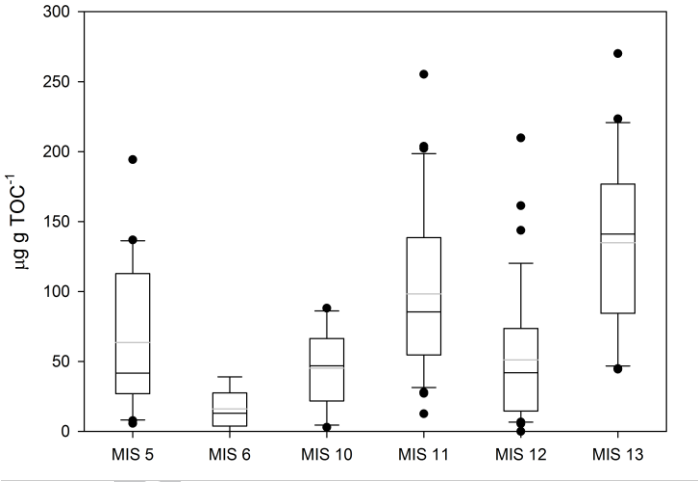

Total organic Carbon (TOC, %) and concentration of C-35 aminoBHPs (ug g-1 sediment) in ODP 1075 Congo Fan sediments.

			Aminotriol	Aminotetrol	Aminopentol	Unsaturated aminopentol	Aminopentol isomer
	depth	*m/z*	714	772	830	828	788
depth (mbsf)	(mcd)	TOC (%)	**I**	**II**	**III**	**III'**	**IV/V**
1.65	1.65	1.8	0.52	-	0.68		-
2.15	2.15	2.8	0.41	0.082	0.092	-	-
2.55	2.55	3.1	0.17	-	0.087	-	-
3.15	3.15	2.7	0.75	-	0.72	-	-
3.65	3.65	3.1	0.44	0.13	0.33	-	-
4.15	4.15	2.6	0.49	-	0.12	-	-
4.65	4.65	3.1	0.35	-	0.14	-	-
5.55	5.55	2.7	0.27	-	0.20	-	-
6.15	6.15	2.9	0.64	-	0.45	-	-
6.65	6.65	3.2	0.64	-	0.30	-	-
7.15	7.15	3.1	0.40	-	0.22	-	-
8.15	8.15	3.0	0.46	0.087	0.092	-	-
8.65	8.65	2.6	0.66	-	0.34	-	-
9.65	9.65	2.2	0.34	-	-	-	-
10.05	10.05	2.0	0.33	0.047	0.21	-	-
10.65	10.65	1.9	0.17	-	0.13	-	-
11.65	11.65	2.2	0.31	-	0.31	-	-
12.05	12.05	2.3	0.57	-	0.75	-	0.058
12.15	12.15	2.2	0.81	0.14	0.36	-	-
12.65	12.65	1.9	1.6	0.24	1.3	-	0.28
13.15	13.15	1.6	1.1	0.20	0.68	-	-
13.55	13.55	1.5	0.62	0.12	0.52	-	-
13.65	13.65	1.4	0.33	-	0.29	-	0.064
14.15	14.15	2.3	1.4	-	0.57	-	-
14.65	14.65	2.4	0.30	-	0.14	-	-
15.15	15.15	2.1	0.29	-	0.16	-	-
15.85	15.85	2.0	1.7	0.45	2.2	-	0.16
16.15	16.15	1.7	1.2	0.16	1.8	-	0.25
16.45	16.45	1.8	1.6	0.47	1.7	0.088	-
16.75	16.75	1.9	1.9	0.48	2.7	0.13	0.44
16.85	16.85	2.0	1.3	0.24	0.99	-	-
17.05	17.05	3.4	1.1	0.15	0.93	-	0.043
17.25	17.25	3.3	2.1	0.27	1.1	-	-
17.35	17.35	3.1	3.6	0.79	2.7	-	0.55
17.75	17.75	2.4	1.2	0.16	0.78	-	-
17.95	17.95	2.0	1.1	0.15	0.51	-	-
18.25	18.25	1.6	1.1	0.16	0.19	-	0.16
18.45	18.45	1.6	0.53	0.13	0.71	-	0.052

18.75	18.75	1.7	0.87	0.27	1.1	-	0.10
18.95	18.95	1.8	0.21	0.077	0.15	-	-
19.05	19.05	2.0	0.23	0.068	0.42	-	0.079
19.25	19.25	3.2	0.15	-	0.10	-	-
19.35	19.35	2.9	0.27	-	-	-	-
19.55	19.55	3.1	0.70	-	0.31	-	-
19.85	19.85	2.5	0.63	-	0.13	-	0.034
20.05	20.05	2.6	0.84	0.14	0.75	-	0.12
20.25	20.25	1.9	0.32	0.060	0.25	-	-
20.55	20.55	2.1	0.66	0.14	0.32	-	0.10
21.15	22.41	2.1	0.20	0.029	0.12	-	-
21.55	22.81	2.2	0.25	-	0.085	-	-
21.65	22.91	2.5	0.14	-	0.13	-	-
22.65	23.91	2.3	1.6	0.26	0.74	-	0.24
24.65	25.91	3.1	2.1	0.25	1.80	-	-
27.15	28.41	2.1	1.0	0.21	0.80	-	-
28.65	29.91	2.5	4.8	0.67	3.4	-	0.28
30.65	31.33	2.8	2.5	0.46	1.7	-	0.11
32.65	33.33	1.9	0.37	-	0.29	-	0.057
34.15	34.83	2.0	1.1	0.12	0.72	-	-
35.55	36.23	1.4	0.55	0.10	0.38	-	-
36.65	37.33	2.4	0.42	0.10	0.10	-	0.23
39.15	39.83	2.1	1.6	0.29	1.6	-	0.18
39.65	40.75	1.8	1.8	0.42	1.6	-	0.054
40.15	41.25	2.7	0.60	-	0.21	-	-
40.55	41.65	2.6	0.36	-	0.074	-	-
40.65	41.75	2.7	0.55	0.13	0.38	-	-
41.15	42.25	2.5	2.6	0.37	1.8	-	-
41.65	42.75	1.8	1.1	0.10	0.79	-	0.048
42.05	43.15	1.6	1.4	0.20	0.77	0.043	0.047
42.15	43.25	1.8	0.40	-	0.27	-	0.13
42.65	43.75	1.8	1.2	0.19	0.49	-	-
43.15	44.25	1.8	0.92	0.14	0.51	-	0.10
43.55	44.65	1.8	1.3	0.30	0.96	-	-
43.65	44.75	1.9	1.4	-	0.99	-	-
44.15	45.25	2.0	1.3	0.26	0.94	-	-
44.65	45.75	1.6	1.7	0.25	0.78	-	-
45.05	46.15	1.9	1.1	0.19	0.77	-	0.049
45.15	46.25	1.8	1.5	0.24	1.3	-	-
45.25	46.35	1.6	1.5	0.34	1.8	0.055	-
45.35	46.45	1.7	0.70	0.18	0.88	-	-
45.55	46.65	2.4	1.6	0.28	1.3	-	0.080
45.65	46.75	2.2	0.93	0.13	0.69	-	-
45.75	46.85	2.5	3.1	0.21	2.3	-	-
45.85	46.95	2.3	1.4	0.26	0.72	-	-
45.95	47.05	3.0	2.5	0.30	1.8	0.14	0.31

46.05	47.15	3.2	4.7	1.5	3.8	-	0.060
46.15	47.25	3.1	3.7	0.44	1.7	-	-
46.25	47.35	3.1	2.2	-	1.1	-	-
46.35	47.45	2.9	4.5	0.38	1.6	-	-
46.45	47.55	3.2	4.9	0.52	2.7	-	-
46.55	47.65	2.9	7.8	1.1	4.7	-	-
46.65	47.75	2.6	1.6	0.32	1.1	-	0.27
46.75	47.85	2.5	3.0	0.32	2.0	-	-
47.05	48.15	1.8	4.3	0.76	3.9	-	-
47.25	48.35	1.7	2.5	0.43	2.0	-	-
47.35	48.45	2.0	4.3	0.56	3.3	-	0.063
47.55	48.65	2.5	2.1	0.36	2.5	-	0.083
47.65	48.75	2.3	1.3	0.25	1.4	-	-
47.75	48.85	2.1	3.5	0.62	3.5	-	-
47.85	48.95	2.2	1.8	0.29	1.8	-	-
47.95	49.05	2.2	3.2	0.60	3.4	0.12	0.086
48.05	49.15	2.1	1.9	0.38	2.3	-	0.047
48.15	49.25	2.1	1.8	0.42	3.1	-	0.21
48.25	49.35	2.4	1.5	0.31	1.8	0.091	0.10
48.35	49.45	2.0	1.3	0.31	1.8	0.068	0.14
48.55	49.65	2.1	0.70	0.19	0.38	-	-
48.75	49.85	2.2	2.3	0.18	0.54	-	-
48.85	49.95	2.2	0.43	-	0.28	-	-
48.95	50.05	2.2	0.79	0.11	0.51	-	-
49.05	50.15	2.1	0.91	0.12	0.66	-	-
49.15	50.25	1.9	0.66	-	0.19	-	-
49.24	50.34	2.0	0.82	0.18	0.30	-	0.10
49.15	51.51	2.0	0.37	0.076	0.23	-	-
49.35	51.71	2.6	0.63	-	0.49	-	-
49.45	51.81	2.3	0.23	0.027	0.25	-	-
49.52	51.88	2.3	0.88	0.081	0.51	-	-
49.65	52.01	2.2	0.48	-	0.15	-	-
49.75	52.11	2.5	0.35	-	0.30	-	-
49.85	52.21	1.9	0.70	0.17	0.63	-	-
49.95	52.31	1.7	0.40	0.040	0.30	-	-
50.05	52.41	2.0	0.78	0.12	0.53	-	-
50.15	52.51	2.6	0.97	-	-	-	-
50.25	52.61	2.3	0.57	0.087	0.40	-	-
50.35	52.71	2.5	1.1	-	0.61	-	-
50.55	52.91	1.7	0.16	-	0.11	-	-
50.65	53.01	2.0	0.53	-	0.21	-	-
50.75	53.11	2.1	0.32	-	0.11	-	-
50.85	53.21	2.3	1.8	0.21	0.90	-	-
50.95	53.31	2.2	2.3	0.24	0.92	-	-
50.95	53.31	2.0	2.4	0.24	1.3	-	0.064
51.15	53.51	2.0	1.0	0.17	0.64	-	-

51.35	53.71	1.9	1.5	0.21	1.3	-	-
51.45	53.81	1.6	1.5	0.24	1.4	-	-
51.55	53.91	1.5	1.6	0.28	1.4	0.061	-
51.65	54.01	1.5	0.60	0.13	0.64	-	-
51.75	54.11	1.8	0.79	0.20	0.50	-	0.12
51.85	54.21	2.1	1.3	0.16	0.74	-	0.045
52.08	54.44	2.7	0.55	0.049	0.42	-	-
52.28	54.64	2.7	1.6	0.21	1.2	-	-
52.38	54.74	3.2	2.1	0.29	2.1	-	-
52.48	54.84	2.8	2.0	0.25	1.4	-	-
52.68	55.04	2.2	0.37	-	0.25	-	-
52.78	55.14	2.7	2.4	0.38	1.6	-	-
52.88	55.24	2.6	2.0	0.26	1.5	-	0.093
52.98	55.34	2.4	4.9	0.76	4.3	-	-
53.08	55.44	2.3	4.1	0.73	3.0	-	-
53.18	55.54	2.6	6.5	0.70	3.0	-	-
53.28	55.64	2.5	3.1	0.43	2.4	-	0.10
53.38	55.74	2.2	2.4	0.05	2.1	-	-
53.62	55.98	3.1	4.9	0.41	2.1	-	0.45
53.72	56.08	3.1	1.8	0.38	1.4	-	-
53.84	56.2	3.3	2.7	0.34	1.1	-	-
53.92	56.28	3.3	7.3	0.42	2.4	-	0.42
54.02	56.38	3.2	1.9	0.17	1.3	-	-
54.12	56.48	3.2	3.5	0.25	1.3	-	0.22
54.22	56.58	2.3	3.9	0.72	3.9	0.071	-
54.34	56.7	2.1	2.8	0.40	2.5	-	0.12
54.42	56.78	1.8	3.7	0.87	3.8	0.14	0.089
54.52	56.88	1.6	3.1	0.47	3.1	0.080	-
54.62	56.98	1.7	3.7	0.40	2.3	-	-
54.72	57.08	1.6	3.4	0.61	2.0	-	-
54.84	57.2	1.7	2.8	0.41	2.5	-	-
54.92	57.28	1.9	4.2	0.55	3.4	-	-
55.22	57.58	2.3	4.3	0.84	3.4	-	-
56.12	58.48	2.0	2.2	0.40	2.5	-	0.12
56.22	58.58	2.3	3.5	0.39	2.3	-	0.080
56.72	59.08	2.9	7.1	0.76	2.5	0.34	0.67
57.22	59.58	3.3	5.4	0.60	1.8	-	-
57.62	59.98	2.0	2.0	0.28	1.7	-	0.27
57.72	60.08	1.9	2.7	0.44	2.4	-	-
58.15	60.51	1.8	2.1	0.35	1.2	-	-
58.65	61.01	1.7	2.5	0.42	2.0	-	-
58.65	62.55	2.2	3.4	0.62	2.0	-	-
59.15	63.05	2.5	1.6	0.23	1.2	-	0.056
60.15	64.05	2.6	2.4	0.36	1.1	-	-
62.2	66.1	3.5	2.6	0.50	1.6	-	0.28
64.1	68	2.7	0.60	0.15	0.29	-	0.083

65.74	69.64	2.5	3.1	0.45	2.2	-	-
66.78	70.68	1.2	0.71	0.22	0.88	-	0.16
67.28	71.18	1.7	0.90	0.15	0.32	-	-
67.83	71.73	2.3	1.1	0.19	0.82	-	0.075
68.15	73.29	2.0	2.3	0.21	0.44	-	0.11
69.05	74.19	2.0	0.16	-	0.061	-	-
71.15	76.29	2.1	1.3	0.17	1.4	-	0.16
73.59	78.73	1.8	0.12	-	0.052	-	-
74.73	79.87	1.7	3.0	0.54	2.1	-	0.060
76.23	81.37	1.6	0.20	0.085	0.11	-	-
77.73	82.87	2.0	0.14	0.039	0.089	-	-
79.62	86	2.0	1.2	0.19	0.87	-	-
81.52	87.9	1.7	0.12	-	0.077	-	-
82.92	89.3	1.9	2.5	0.38	1.1	-	0.091
84.25	90.63	1.5	1.9	0.21	1.4	-	0.18
86.4	92.78	1.0	0.24	0.074	0.19	-	-
87.3	93.68	1.8	0.28	0.063	0.27	-	-
88.05	95.55	2.1	0.24	-	0.066	-	-
89.51	97.01	2.3	0.63	0.11	0.34	-	-
92.13	99.63	1.9	1.8	0.24	0.75	-	-
93.65	101.15	2.7	1.0	0.075	0.48	-	0.11
94.13	101.63	1.1	0.86	0.16	0.36	-	-
95.13	102.63	2.5	1.3	-	0.40	-	-
96.03	103.53	1.1	0.27	0.074	0.33	-	0.077
97.65	106.93	2.5	1.8	0.22	1.3	-	0.078
100.55	109.83	2.8	2.2	0.32	1.0	-	-
101.75	111.03	1.0	1.1	0.22	0.93	-	-
103.71	112.99	2.1	0.61	-	0.18	-	-
106.31	115.59	1.1	1.8	0.25	1.1	-	0.44
108.15	119.02	1.3	4.6	0.66	2.2	0.092	-
111.55	122.42	1.2	0.37	0.10	0.22	-	0.067
113.15	124.02	0.86	0.69	0.11	0.44	-	0.22
114.55	125.42	1.5	2.4	0.44	1.7	-	0.20
115.65	126.52	1.2	0.43	0.11	0.22	-	0.24
115.7	126.97	1.2	1.2	0.19	1.4	-	-
116.7	127.97	1.7	2.2	0.27	1.8	0.044	-
117.2	128.47	0.86	1.6	0.25	1.6	0.029	0.11
117.7	128.97	0.74	0.04	-	0.018	-	-
118.7	129.97	1.4	0.20	-	0.20	-	-
119.7	130.97	0.77	1.3	0.19	1.30	0.023	0.038
120.7	131.97	1.9	1.7	0.21	0.66	0.094	-
121.7	132.97	0.87	2.0	0.39	2.40	-	0.13
122.7	133.97	1.4	1.9	0.27	1.20	0.052	-
123.7	134.97	1.5	1.6	0.27	0.93	-	-
124.7	135.97	0.82	1.1	0.20	0.84	-	-
125.67	136.94	1.7	1.3	0.18	0.90	-	-

125.88	139.09	1.7	0.14	-	0.10	-	-
126.86	140.07	0.87	0.79	0.17	1.10	0.035	0.061
127.88	141.09	2.1	1.4	0.18	0.40	-	0.20
128.98	142.19	1.3	1.7	0.18	0.68	-	-
130.03	143.24	2.2	1.6	0.17	0.68	-	-
131.01	144.22	0.91	1.7	0.27	0.83	-	0.063
132.03	145.24	1.3	1.8	0.28	1.5	0.037	0.10
133.03	146.24	1.4	2.3	0.40	2.5	0.068	-
134.01	147.22	1.7	1.4	0.20	0.89	-	-
134.53	147.74	1.2	2.8	0.42	2.6	0.068	0.17
134.74	149.53	0.87	0.79	0.18	0.97	0.031	0.076
135.7	150.49	2.7	3.0	0.42	2.3	0.051	0.18
136.7	151.49	1.1	1.8	0.32	1.1	-	-
137.7	152.49	1.6	1.7	0.18	0.65	-	-
138.7	153.49	1.6	2.6	0.42	2.4	0.040	0.12
139.7	154.49	2.0	2.2	0.31	1.5	0.041	0.052
140.7	155.49	1.3	1.9	0.24	1.4	-	0.028
141.7	156.49	1.3	1.6	0.29	1.1	-	-
142.7	157.49	1.9	1.4	0.19	0.99	0.022	0.033
143.7	158.49	1.6	1.5	0.23	1.4	-	0.23
144.2	159.83	1.1	1.3	0.16	0.72	-	-
145.2	160.83	1.2	1.9	0.34	1.9	0.045	0.16
146.2	161.83	1.9	2.0	0.25	1.8	-	0.074
147.2	162.83	1.4	1.9	0.27	0.60	0.019	0.36
148.2	163.83	1.7	1.5	0.23	0.96	0.026	0.21
149.2	164.83	2.0	2.9	0.28	0.83	-	-
150.2	165.83	0.85	2.4	0.40	1.6	0.030	-
151.2	166.83	2.0	1.3	0.16	0.96	0.027	0.032
152.2	167.83	0.94	2.1	0.38	2.1	0.061	0.27
153.2	168.83	2.3	2.4	0.30	1.2	-	-
154.16	169.79	1.3	1.4	0.25	1.5	-	-
154.2	171.55	2.5	2.5	0.30	1.4	-	0.15
155.2	172.55	1.8	1.8	0.24	1.0	-	-
156.2	173.55	2.0	1.4	0.14	0.80	-	-
157.2	174.55	1.8	2.2	0.27	0.89	-	-
158	175.35	1.5	1.6	0.17	0.74	-	-
159	176.35	1.4	1.2	0.15	0.61	-	-
159.93	177.28	1.2	0.67	0.13	0.40	-	-
160.93	178.28	2.2	1.5	0.13	0.52	-	-
161.93	179.28	1.3	1.2	0.15	0.63	-	-
162.93	180.28	2.6	1.6	0.15	0.67	-	-
163.18	182.63	1.2	1.4	0.22	0.76	-	-
164.2	183.65	1.7	2.7	0.33	1.9	-	0.11
165.2	184.65	1.6	2.3	0.27	0.89	-	-
166.2	185.65	1.5	2.1	0.36	1.2	-	-
167.2	186.65	1.7	1.5	0.25	1.7	-	0.043

168.2	187.65	2.1	1.3	0.16	0.77	-	0.11
169.2	188.65	2.7	1.8	0.21	1.1	-	0.029
170.2	189.65	1.3	1.5	0.28	1.6	-	0.20
171.2	190.65	2.4	1.4	0.14	0.93	-	-
172.2	191.65	1.1	1.7	0.27	0.76	-	0.16
173.12	192.57	3.5	1.6	0.15	0.94	-	-
174.21	194.83	1.8	1.6	0.19	1.1	-	0.042
175.11	195.73	1.5	1.8	0.25	1.0	-	-
176.11	196.73	2.1	2.2	0.20	0.74	-	-
177.11	197.73	1.5	0.65	0.08	0.27	-	0.053
178.11	198.73	1.9	2.2	0.30	1.7	-	0.10
179.11	199.73	2.3	2.3	0.28	1.6	-	-
180.11	200.73	2.6	1.7	0.19	1.1	-	0.054
181.22	201.84	1.3	1.9	0.27	1.3	-	0.22
182.18	202.8	1.9	1.4	0.13	0.29	-	0.10
183	203.62	1.2	1.1	0.17	0.93	-	0.077
182.7	205.25	2.7	1.5	0.18	0.80	-	0.22
183.68	206.23	1.7	1.8	0.25	0.74	-	-
184.68	207.23	1.5	1.4	0.15	0.84	-	-
185.68	208.23	1.6	0.94	0.14	0.72	-	-
186.7	209.25	2.2	2.1	0.29	1.0	-	-
187.76	210.31	1.4	1.5	0.23	1.4	0.053	0.092
189.69	212.24	0.87	1.3	0.14	0.59	-	-
190.7	213.25	2.0	1.3	0.15	0.45	-	-
191.7	214.25	1.8	1.8	0.29	0.67	-	-
191.8	217.28	2.0	1.6	0.17	0.85	-	0.11
192.7	218.18	2.4	1.7	0.17	0.84	-	0.10
193.68	219.16	2.6	1.1	0.15	0.62	-	-
194.69	220.17	1.5	0.90	0.09	0.59	-	-
195.68	221.16	3.2	1.3	0.10	0.47	-	-
196.78	222.26	1.2	0.7	0.10	0.44	-	-
197.69	223.17	2.7	1.4	0.12	0.62	-	-
198.69	224.17	1.2	0.91	0.11	0.24	-	0.13
199.69	225.17	1.8	0.95	0.093	0.24	-	-
200.69	226.17	2.2	1.5	0.16	0.91	-	-
201.25	226.73	2.5	1.8	0.19	0.70	-	-